

Learning Reinforced Agents with Counterfactual Simulation for Medical Automatic Diagnosis

Junfan Lin, Ziliang Chen, Xiaodan Liang, Keze Wang, and Liang Lin

Abstract—Medical automatic diagnosis (MAD) aims to learn an agent that mimics the behavior of a human doctor, i.e. inquiring symptoms and informing diseases. Due to medical ethics concerns, it is impractical to directly apply reinforcement learning techniques to solving MAD, e.g., training a reinforced agent with the human patient. Developing a patient simulator by using the collected patient-doctor dialogue records has been proposed as a promising approach to MAD. However, most of these existing works overlook the causal relationship between patient symptoms and disease diagnoses. For example, these simulators simply generate the “not-sure” response to the inquiry (i.e., symptom) that was not observed in one dialogue record. As a result, the MAD agent is usually trained without exploiting the *counterfactual reasoning* beyond the factual observations. To address this problem, this paper presents a propensity-based patient simulator (PBPS), which is capable of facilitating the training of MAD agents by generating informative counterfactual answers along with the disease diagnosis. Specifically, our PBPS estimates the propensity score of each record with the patient-doctor dialogue reasoning, and can thus generate the counterfactual answers by searching across records. That is, the unrecorded symptom for one patient can be found in the records of other patients according to the propensity score matching. A progressive assurance agent (P2A) can be thus trained with PBPS, which includes two separate yet cooperative branches accounting for the execution of symptom-inquiry and disease-diagnosis actions, respectively. The disease-diagnosis predicts the confidence of disease and drives the symptom-inquiry in terms of enhancing the confidence, and the two branches are jointly optimized with benefiting from each other. In the experiments, our trained agent achieves the new state-of-the-art under various experimental settings and possesses the advantage of sample-efficiency and robustness compared to other existing MAD methods.

Index Terms—Medical automatic diagnosis, Counterfactual casual reasoning, Reinforcement learning, Neural networks.

1 INTRODUCTION

Medical automatic diagnosis (MAD) aims to learn an agent which role-plays the human doctor to interact with the patient, for information collecting and preliminarily diagnosing. The task increasingly grasps the attention of researchers because of its significant industrial potential [1]. Similar to other task-oriented dialogue tasks, e.g. movie ticket/restaurant booking, online shopping and technical support [2], [3], [4], [5], MAD is composed of a sequence of dialogue-based interactions between the user and the agent, which can be formulated as a Markov decision process and resolved by reinforcement learning (RL) [6], [7]. In particular, RL regularly encourages the agent in trial and error to search the optimal policy. However, the trial-and-error strategy for learning a MAD agent in real-life scenarios is impractical since it requires the agent to misdiagnose human patients frequently, violating medical ethics.

Instead of interacting with the human patient, developing a *patient simulator* by using the collected patient-doctor dialogue records collected from the real-life has been proposed as a promising workaround to MAD [6], [7]. In these

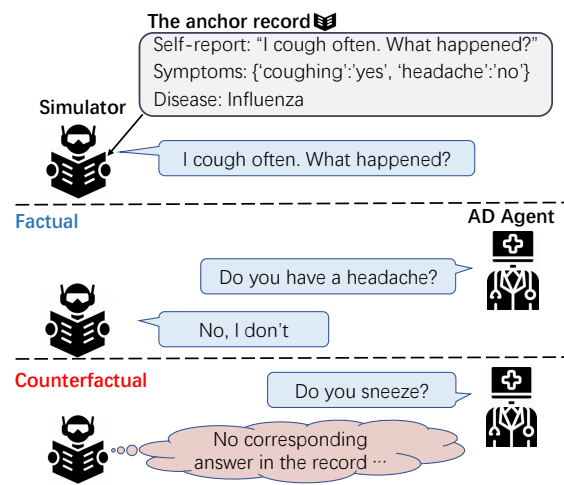


Fig. 1: The demonstration of the counterfactual symptom inquiry problem. The patient simulator chooses a record as the anchor record and gives its self-report to start a diagnosis process. Then, the simulator answers the *factual symptom inquiries* which are already observed in the anchor record. This simulator would fail to answer the *counterfactual symptom inquiries* about the unobserved symptoms.

- J. Lin, Z. Chen, and L. Lin was with the School of Data and Computer Science, Sun Yat-sen University, Guangzhou, Guangdong, China, 510006.
E-mail: linjf8@mail2.sysu.edu.cn, c.ziliang@yahoo.com, lin-liang@ieee.org.
- X. Liang was with the School of Intelligent Systems Engineering, Sun Yat-sen University, Guangzhou, Guangdong, China, 510006.
E-mail: xdliang328@gmail.com.
- K. Wang was with the Departments of Statistics and Computer Science, University of California, Los Angeles, USA.
E-mail: kezewang@gmail.com

works, researchers train the MAD agent using a patient simulator which chooses a dialogue record (anchor record) from the dialogue dataset, and then answers the inquiries according to the anchor record. Unfortunately, the dialogue record is passively observational, that's, the record solely contains a fraction of inquiry-answer pairs. These inquiry-answer pairs are *factual* since they have already happened.

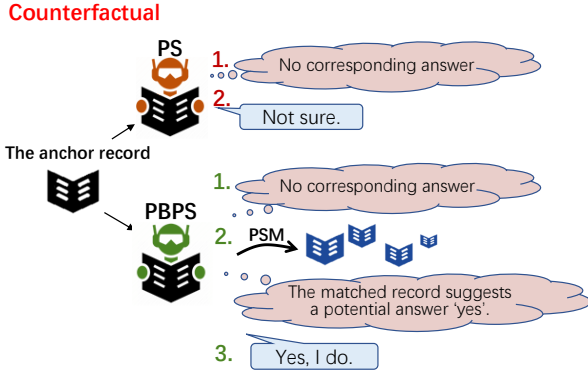


Fig. 2: The difference between the original patient simulator (PS) and our propensity-based patient simulator (PBPS) in dealing with a *counterfactual symptom inquiry*. Confronting a *counterfactual symptom inquiry* (step 1), PS would answer with ‘not sure’ (step 2) while PBPS would estimate the potential existence of the symptom using propensity score matching (PSM) (step 2) and answer according to the deduced symptom existence (step 3).

The patient simulator answers inquiries solely based on the factual information would fail to answer the inquiry about the unobserved symptom, namely, the *counterfactual symptom inquiry*. The difference between factual and counterfactual symptom inquiry is shown in Fig. 1. The problem of the counterfactual symptom inquiry brings in the major gap between the patient simulator and the human patient.

As many anthropologists [8], [9] point out, the decisive ingredients for human-kind to achieve global domination is the ability to picture the environment mentally, reason within that mental representation, intervene it by imagination and finally answer interventional questions like “What if I open the box?” and counterfactual questions like “What if the electric light had not been invented?”. J. Pearl and M. A., Hernán [10], [11] postulated that it’s critical to equip learning machines with causal reasoning tools to achieve accelerated learning speeds as well as human-level performance. Therefore, it’s essential to introduce the ability of retrospective reasoning to the patient simulator to close the gap between the patient simulator and the human patient.

Unfortunately, the counterfactual inquiry problem is severely underestimated by existing works [6], [7]. Without exploiting the causal relationship between patient symptoms and disease diagnoses, these works subjectively assert that the human patients were not sure about the unobserved symptoms and cope with the substantial counterfactual symptom inquiries by making the simulator answer with a ‘not-sure’ response as shown in Fig. 2. This manner severely violates the reality in a patient-doctor dialogue, and the considerable amount of uninformative (with ‘not-sure’ words) and disease-unrelated (not helpful in revealing the symptom-disease relation) answers bring about more difficulty and uncertainty to diagnose.

Inspired by the success of causality [12], [13], [14] that it is possible to estimate the potential outcomes given passive observational data, we attempt to mine the potential existences of the unobserved symptoms by introducing the causal inference technique, i.e., *Propensity Score Matching* (PSM) [15], [16], into the patient simulator to resolve the above-mentioned problem. Specifically, our proposed

propensity-based patient simulator (PBPS) train a neural network to estimate the propensity score of each record according to the learned embeddings of their observed symptoms and the ground-truth diseases. The records with the similar propensity scores are prone to have similar symptoms and diseases, and therefore the potential existences of the unobserved symptoms in one record can be deduced from the other with similar propensity score, as shown in Fig. 2. Through mining the passive observational data in such a collaborative representation manner, to the best of our knowledge, we are the first one to propose a simple yet concise paradigm to apply reinforcement learning with only passive observational data.

Since the original patient simulator only generates an informative answer when the inquiry is factual, the information in the early phase of the diagnosis process is usually insufficient to inform a disease. In this way, existing works consider the disease-diagnosis is non-overlapped with but successive to the symptom-inquiry process, and unify them into a single policy network. However, with more informative and disease-related answers from PBPS per step, an agent can learn a policy for symptom-inquiry and a diagnoser for disease-diagnosis separately, to make and adjust the disease estimation interleaving the symptom-inquiry process. Learning a diagnoser separately contributes to making better use of data to form a fast-converging (sample-efficient) training process and allowing specific handling to the diagnosis, to achieve a more robust diagnosis.

To this end, we also propose a progressive assurance agent (P2A) which consists of two separate yet cooperative branches, i.e., diagnosis branch and inquiry branch, inspired by the dual-process theory in neuroscience [17], [18]. In [17], [18], neuroscientists suggested that a decision is produced by two separate yet cooperative processes in the human brain. One is fast but impulsive while the other is slow but rational. In P2A, the ‘slow but rational’ diagnosis branch estimates the disease and its confidence at each step and drives the ‘fast but impulsive’ inquiry branch in terms of enhancing the confidence progressively until the agent is confident enough to inform the disease.

We name our RL framework, consisting of PBPS and P2A as Counterfactual-Simulated MAD (CSMAD). The main contributions of this work are two-fold. i) We present a novel patient simulator PBPS that takes the advantages of PSM to tackle the problem of counterfactual symptom inquiry, and may also inspire other RL tasks with passive observational data; ii) Equipped with PBPS, we propose a novel MAD agent, P2A, inspired by the dual-process theory in neuroscience, which additionally models the confidence to drive the symptom-inquiry, achieving safer and more reliable diagnoses. Experimental results demonstrate that PBPS can generate more informative and disease-related answers, and P2A achieves the new state-of-the-arts under various settings and possesses the advantage of sample-efficiency and robustness compared to other existing MAD methods.

The remainder of this paper is organized as follows. Section 2 briefly reviews the existing MAD agents based on reinforcement learning and related techniques. Section 3 introduces the background of reinforcement learning and the counterfactual symptom inquiry. Section 4 presents the details of the proposed framework CSMAD (PBPS + P2A).

Section 5 presents the experimental results and human evaluation on two public benchmarks with comprehensive evaluation protocols, as well as comparisons with competing alternatives. Finally, Section 6 concludes this paper.

2 RELATED WORK

Medical automatic diagnosis (MAD) have gathered considerable attention in recent years. [1], [19], [20] have been committed to improving diagnostic performance in large simulated data. [7] first did experiments on real-world data by DQN [21], [22], [23] while [6] proposed an end-to-end model, KR-DQN, for MAD guided by knowledge graph. Different from these works, our proposed agent estimates the diagnosis confidence to drive the symptom-inquiry and provide a stop mechanism (used to indicate when to stop inquiring). There are plenty of works studying how to combine uncertainty and exploration [24], [25], [26], [27], [28]. However, these works didn't consider using the uncertainty to provide a stop mechanism for sequential decision making.

However, patient simulators in [6], [7] adopted patient-doctor conversation records [29], [30] to train the RL agents, which typically lack the symptom complexity of human interlocutors and the trained agent is inevitably affected by biases in the design of the simulator [31]. [32] incorporated a model of the environment into the dialogue agent to generate simulated user experience, which however is prone to generate data with similar characteristics as the original data [33]. A reinforced agent who takes actions to explore might receive a false response from the simulator as the simulator only known how to answer according to what is in the record. Therefore the patient simulator is required to estimate the potential symptom existence to develop an active environment. [12], [13] proposed the potential outcomes of actions could be inferred from the passive observational data through the matching methods [14]. To overcome the *lack of overlap* issue during matching [16], the most widely adopted matching as weighting methods specify the compact representation in estimating the *propensity score* [15].

3 BACKGROUND

A diagnosis record consists of a self-report, symptom existences $\mathbf{y} = [y_a]_{a=1}^n \in \{-1, 0, 1\}^n$ (-1 for 'no', 1 for 'yes', 0 for the unobserved symptom) and a ground-truth disease $d \in [1, m]$, where n is the number of symptoms and m is the number of diseases, as shown in Fig. 1.

MAD task has been formulated as a Markov decision process (MDP) problem [6], [7], and is denoted by using the tuple $\mathcal{M} = \{\mathcal{S}, \mathcal{A}, \mathcal{P}, \mathcal{R}, \gamma\}$. $\mathcal{S} \subseteq \mathbb{R}^n$ is the state space, in which, $\mathbf{s}_t \in \mathcal{S}$ maintains the values of all mentioned symptoms (-2 is the default value for the unvisited symptom, -1 for 'no', 0 for 'not-sure' and 1 for 'yes') up to time t . And $\mathcal{A} \subseteq \mathbb{N}^{n+m}$ represents the action spaces of the agent, in which $a \in \mathcal{A}$ is either the symptom inquiry or disease informing. $\mathcal{R} : \mathcal{S} \times \mathcal{A} \rightarrow \mathbb{R}$ is the reward function which measures diagnosis progress. $\mathcal{P} : \mathcal{S} \times \mathcal{A} \rightarrow \mathcal{S}$ is the transition dynamics. The initial state is initialized by the symptoms mentioned in the self-report. And $\gamma \in [0, 1)$ is a

discount factor. We wish to solve for a policy of the form $\pi : \mathcal{S} \rightarrow \mathcal{A}$, which maximizes the expected sum of rewards: $\eta(\pi) = \mathbb{E}_{\pi, \mathcal{M}}[\sum_{t=0}^{\infty} \gamma^t r_t]$.

3.1 Motivation

3.1.1 Counterfactual symptom inquiry

In building a simulator, a diagnosis record demonstrates how to answer the agent's symptom inquiry a . In each record, the simulator can access both to the symptom existences \mathbf{y} and the disease d . Furthermore, the simulator can answer a factual symptom inquiry a according to y_a ($y_a \neq 0$), while failing to answer a *counterfactual symptom inquiry* a unobserved in the record (i.e. $y_a = 0$), as demonstrated in Fig. 1. To solve this problem, the simulator is required to estimate potential symptom existence Y_a of the inquired symptom a when given the record (\mathbf{y}, d) .

The definition of potential symptom existence resembles the spirit of the potential outcome [12], [13] (referred to Appendix). In our context, it denotes the symptom existence of the inquired symptom. In this way, if the potential symptom existence can be estimated, the simulator can follow it to answer the factual/counterfactual symptom inquiry. This potential symptom existence could be estimated by the matching method [14] in causal inference. The matching method is popular in estimating the potential outcomes of actions given passively observational data. The goal of the matching method is to construct a subset of the population in which the *covariates* have the same distribution in different actions, and thus the potential outcomes can be regarded as the same in the population. But as the covariates are typically severely sparse making the samples terribly difficult to match, propensity score matching [15], [16] is developed to tackle this *lack of overlap* issue by estimating a more compact representation for matching, i.e., the propensity score $P(\text{action}|\text{covariates})$.

In MAD task, given a record with covariates (\mathbf{y}, d) and a symptom inquiry a , the propensity score is $P(Y_a|\mathbf{y}, d)$, where Y_a is the potential symptom existence. Assuming symptoms are solely dependent on the disease, the propensity score with all symptom inquiries is $P(\mathbf{Y}|\mathbf{y}, d) = \prod_a P(Y_a|\mathbf{y}, d)$. The mathematical explanation about why the PSM method works in counterfactual symptom inquiry is presented in the Appendix A.

4 COUNTERFACTUAL-SIMULATED MAD

In this section, we describe our Counterfactual-Simulated MAD (CSMAD) comprised of the propensity-based patient simulator (PBPS) and the progressive assurance agent (P2A).

4.1 Propensity-based Patient Simulator

4.1.1 Propensity score modeling

As introduced in the previous section, PSM method aims to estimate the propensity score $P(\mathbf{Y}|\mathbf{y}, d)$ of each record to generate effective answers. We use multilayer perceptron (MLP) $f_{\phi_P}(\cdot)$ to model $P(\mathbf{Y}|\mathbf{y}, d)$ by reducing the cross-entropy (CE) loss $(f_{\phi_P}(\mathbf{y}, d), \mathbf{y})$, where ϕ_P denotes the parameter of the network. We employ the self-supervised

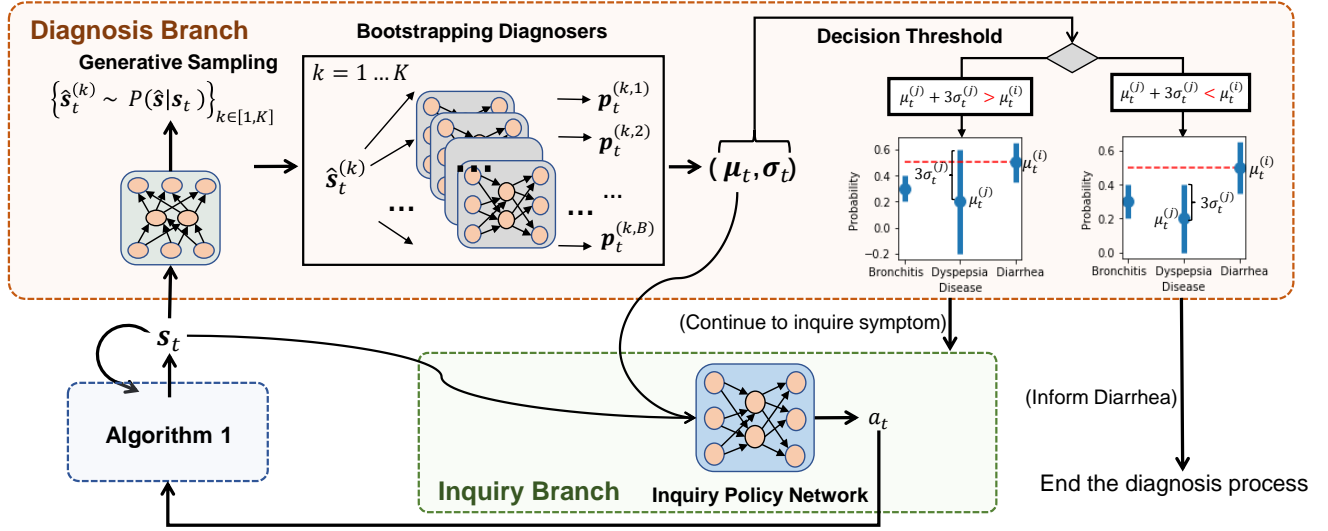


Fig. 3: An overview of our P2A. The diagnosis branch takes s_t to draw K final states which are fed into the B bootstrapping diagnosers to obtain the expectation and deviation. P2A keeps inquiring symptoms of the patient simulator, until the diagnosis meets the decision threshold.

strategy to train the $f_{\phi_P}(\cdot)$ to estimate the potential symptom existence Y_a of any symptom inquiry a . Particularly, we mask off some of \mathbf{y} with binary mask \mathbf{m}^1 and train $f_{\phi_P}(\cdot)$ to reconstruct \mathbf{y} given the masked \mathbf{y} and d . The reconstruction target is

$$\min_{\phi_P} \sum_{i=1}^N \sum_{a=1, y_a \neq 0}^n \sum_{\mathbf{m}} \text{CE}(f_{\phi_P}(\mathbf{y}^{(i)} \odot \mathbf{m}, d^{(i)})_a, y_a^{(i)}). \quad (1)$$

After training, we adopt the output of the second-to-last fully-connected layer as the propensity score, $f_{\phi_P}(\cdot)$, because its dimension is much smaller and information is more compact, in comparison to the last.

4.1.2 Potential existence of symptoms estimation

Given an anchor record p , we show how the simulator estimates the existence of an unobserved symptom a . Our simulator explores all records $\{q\}$ that have the same disease i.e. $d^{(q)} = d^{(p)}$, and also have a in their observed symptoms, i.e. $y_a^{(q)} \neq 0$. It eliminates the irrelevant information of the inquired symptom and disease. The similarity weight of a record q w.r.t to p is formulated as

$$P(q|p, a) \propto \mathbb{I}((d^{(q)} = d^{(p)}) \wedge (y_a^{(q)} \neq 0)) \times e^{-\frac{\|f_{\phi_P}^{(p)} - f_{\phi_P}^{(q)}\|^2}{\sigma^2}}, \quad (2)$$

where $e^{-\frac{\|f_{\phi_P}^{(p)} - f_{\phi_P}^{(q)}\|^2}{\sigma^2}}$ denotes a nonparametric density kernel [34] ($\sigma > 0$ indicates a standard deviation of the propensity scores), implying that if a patient q is more similar to the patient p in their propensity scores, their existences of symptoms are more probably similar. $\mathbb{I}(\cdot)$ is an indicator function that returns 1 if the propositional logic formula in the bracket is satisfied, otherwise returns 0. Then the patient simulator can sample a record $q' \sim P(q|p, a)$, and use its

1. The binary mask is generated according to the order of the symptoms in the dialogue record. An entry in the mask can be set to be 0 only if the entries of its subsequential symptoms in the record are set to be 0.

Algorithm 1 Propensity-based patient simulator (PBPS): $\mathcal{P}_{\text{PBPS}}(s_t, a_t; p)$

Input: s_t, a_t , anchor record p with the self-report and $(\mathbf{y}^{(p)}, d^{(p)})$

Output: s_{t+1}

- 1: **if** $t = -1$ **then**
- 2: Initialize $s_0 \leftarrow [-2, -2, \dots, -2]$ with the size of n ,
- 3: Let $s_{0,a} \leftarrow y_a$, for each a parsed from the self-report
- 4: Return s_0
- 5: **else**
- 6: Initialize $a \leftarrow a_t, s_{t+1} \leftarrow s_t, q' \leftarrow p$
- 7: **If** $((y_a = 0) \wedge (s_{t+1,a} = -2))$, **sample** $q' \sim P(q|p, a)$ **according to Equ.(2)**.
- 8: Update state s_{t+1} by $s_{t+1,a} \leftarrow y_a^{(q')}$
- 9: Return s_{t+1}

symptom existence $y_a^{(q')}$ as the potential symptom existence of the anchor record. More details are in Appendix A.

The MDP transition $\mathcal{P}_{\text{PBPS}}$ of our patient simulator is concluded in Alg.1, in which, the statement in bold (line 7) is the difference of PBPS from the original patient simulator \mathcal{P}_{PS} . As shown in the running example in Fig. 4 (step 3-5), PBPS would conduct PSM in the record base when the anchor record doesn't include the answer of the inquiry.

4.2 Reconfiguring MAD Agents with PBPS

The informative and disease-related answers from PBPS encourage an agent to learn a disentangled diagnoser from the policy, which would improve the diagnosis performance of the agent by making better use of the data and allowing special handling on the diagnosis.

4.2.1 Disentangling Inquiry and Diagnosis

Since the answers from the original patient simulator would be informative only when the inquiries are factual, the state s_t is prone to be insufficient to estimate the disease in the

early diagnosis process. It leads the MAD agent to estimate the disease only after the symptom-inquiry process, therefore the actions of symptom inquiry and disease informing can be assigned to a single policy [6], [7]. Conversely, with PBPS, an agent is able to gather informative response per step. Hence, it is encouraged to learn a diagnoser to make and adjust its disease estimation along the symptom-inquiry process parallelly. This disentanglement manner is also supported by the dual-process theory in neuroscience [17]. A popular opinion in neuroscience suggests that there might be two separate yet cooperative processes for decision making in human brain [17]. One is fast but impulsive, and the other is slow but rational. Especially, the most recent “*as soon as possible*” effect [18] shows that the impulsive process is dependent on the reward as well as *getting something as soon as possible*.

Training a diagnoser disentangled from the symptom inquiry policy is beneficial. Firstly, the original policy network might arise unstable diagnosis since its diagnosing strategy is sensitive to the order of the symptoms inquired. Specifically, the original policy network might diagnose different diseases with different inquiry orders (e.g., “ $A \rightarrow B \rightarrow C$ ” and “ $A \rightarrow C \rightarrow B$ ”) since it learns to diagnose by a sequence of states in MDP. However, the disentangled diagnoser would make the same diagnosis since it diagnoses with a set of states $\{A, B, C\}$. Secondly, the disease-diagnosis component of original policy network would receive feedback only at the end of the diagnosis process, meaning that the improvement of the disease-diagnosis of the previous states have to rely on feedback propagating from the end of the process, which is prone to be unstable and sample-inefficient [1]. Disentangled diagnoser learns to diagnose for each state with direct supervision, making full use of the data and stabilizing the learning process.

4.3 Progressive Assurance Agent

Inspired from the previous discussion, we propose a *Progressive Assurance Agent* (P2A) consisting of two separate yet cooperative branches for symptom-inquiry and disease-diagnosis, as shown in Fig. 3. In P2A, the ‘fast but impulsive’ inquiry branch inquires symptoms to get s_t from PBPS to maximize the sum of rewards while the “slow but rational” diagnosis branch models the $P(d|s_t)$ to estimate the disease and its confidence according to s_t per step until it’s confident enough (satisfying *Decision Threshold*) to inform a disease. The inquiry branch is driven by the diagnosis branch to inquire symptoms that increase the confidence in order to *meet decision threshold as soon as possible*. More details are provided in Appendix B.

4.3.1 Diagnosis Branch

Since what the agent cares is to inform the correct disease with the final state \hat{s} which is the state at the end of the whole diagnosis process, the accuracy of $P(d|\hat{s})$ is more important than the accuracy of $P(d|s_t)$. Rather than directly modeling $P(d|s_t)$, we choose a two-step model for $P(d|s_t) = \sum_{\hat{s}} P(d|\hat{s})P(\hat{s}|s_t)$, and we train generative sampler $f_{\phi_G}(\cdot)$ and discriminative diagnoser $f_{\phi_B}(\cdot)$ for $P(\hat{s}|s_t)$ and $P(d|\hat{s})$ respectively. Moreover, training the two-step model can also encourage the modeling of the diagnosis

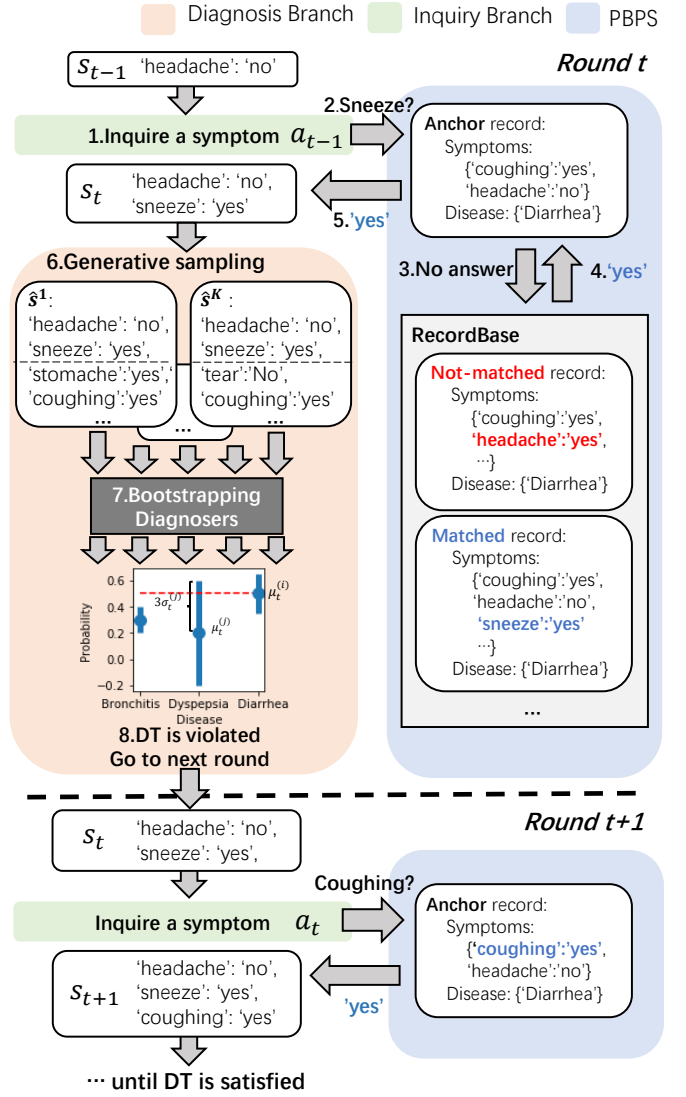


Fig. 4: An intermediate running example of our proposed framework. The left side is the execution of P2A and the right side is of PBPS. The process would continue iteratively until the proposed Decision Threshold is met.

confidence. [26] showed that the reconstruction model like $f_{\phi_G}(\cdot)$ could map out-of-distribution samples to in-distribution samples. Therefore we can only model the in-distribution confidence with $f_{\phi_B}(\cdot)$. We adopt the bootstrapping method to train $f_{\phi_B}(\cdot)$ as it’s known as the most successful and stable method to estimate the in-distribution confidence [26].

Generative sampler is aimed at predicting the final state \hat{s} from the current state s_t . Therefore, we model it as a generative problem. ϕ_G is the parameter of the generator $f_{\phi_G}(\cdot)$, whose target is defined with cross-entropy:

$$\min_{\phi_G} \sum_{i=1}^N \sum_{a=1, s_i, a \neq -2}^n \sum_{\mathbf{m}} \text{CE}(f_{\phi_G}(s_i \odot \mathbf{m})_a, s_{i,a}), \quad (3)$$

where \mathbf{m} is the binary mask constructed in the same way as Equ. (1), and the target for f_{ϕ_G} is to recover the masked information.

Algorithm 2 Progressive Assurance Agent (P2A)

Input: Initial policy π_θ , target policy parameters $\theta_{\text{targ}} = \theta$, final state estimator parameters ϕ_G , B bootstrapping diagnosers parameters ϕ_B , empty replay buffer \mathcal{D}_Q and records buffer \mathcal{D}_C .

- 1: **for** episode = 1, **E do**
- 2: Get one anchor record p to obtain the initial state s_0 according to the self-report
- 3: **for** $t = 0, T$ **do**
- 4: Sample the final states: $\{\hat{s}^{(k)} \sim f_{\phi_G}(s_t), k \in [1, K]\}$
- 5: Forward to bootstrapping diagnosers: $\mathbb{P}_t = \{f_{\phi_B}(\hat{s}^{(k)}, k \in [1, K])\} = \{\mathbf{p}_t^{(k,b)}, k \in [1, K], b \in [1, B]\}$
- 6: Calculate the statistics $\boldsymbol{\mu}_t, \boldsymbol{\sigma}_t$ of \mathbb{P}_t
- 7: **if** $(\epsilon < p \sim U(0, 1)) \wedge (t \neq T)$ **then**
- 8: Inquire symptom: $a_t = s \sim U\{1, N\}$ s.t. $s_{t,s} = -2$
- 9: **else if** $\text{DT}(\boldsymbol{\mu}_t, \boldsymbol{\sigma}_t) \vee (t = T)$ **then**
- 10: Inform disease: $a_t = (\max_i \mu_t^{(i)}) + N$ to end the diagnosis process
- 11: Store records $(s_t, d^{(p)})$ in \mathcal{D}_C and then start a new episode
- 12: **else**
- 13: Request symptom: $a_t = \max_a Q(s_t, \boldsymbol{\mu}_t, a; \theta)$
- 14: Interact with the patient simulator and update state $s_{t+1} = \mathcal{P}_{\text{PBPS}}(s_t, a_t; p)$ according to Alg. 1
- 15: Store transition $(s_{t-1}, \boldsymbol{\mu}_{t-1}, a_{t-1}, s_t, \boldsymbol{\mu}_t)$ in \mathcal{D}_Q
- 16: **if** time to update **then**
- 17: Sample minibatch from \mathcal{D}_Q and update θ and θ_{targ} according to Equ. (8) and Equ. (9)
- 18: Sample B minibatches from \mathcal{D}_C with replacement to update ϕ_G and ϕ_B according to Equ. (3) and Equ. (4)

Bootstrapping diagnosers are trained to diagnose using the final state of the dialogue. The training final states are sampled from the data buffer with replacement. The target of diagnoser i with parameter $\phi_{B,i}$ is

$$\min_{\phi_{B,i}} \sum_{(\hat{s}, d)} \text{CE}(f_{\phi_{B,i}}(\hat{s}), d) \quad \text{s.t. } \forall i \in [1, B]. \quad (4)$$

As shown in the overview (Fig. 3) and running example (step 6 and 7 in Fig. 4), the Monte Carlo sampling is applied by obeying the generative model $f_{\phi_G}(s_t)$ to sample K possible final states $\{\hat{s}^{(k)}\}_{k=1}^K$. These states are then fed into B bootstrapping diagnosers, resulting in a final disease probability set $\{\mathbf{p}_t^{(k,b)}\}_{k=1, b=1}^{K, B}$.

The final disease probability set is then used to calculate the expectation $\boldsymbol{\mu}_t = [\mu_t^{(1)}, \dots, \mu_t^{(m)}]$ and standard deviation $\boldsymbol{\sigma}_t = [\sigma_t^{(1)}, \dots, \sigma_t^{(m)}]$ of diseases:

$$\boldsymbol{\mu}_t = \frac{1}{KB} \sum_{b=1}^B \sum_{k=1}^K \mathbf{p}_t^{(k,b)}, \quad \boldsymbol{\sigma}_t^2 = \frac{1}{KB} \sum_{b=1}^B \sum_{k=1}^K (\mathbf{p}_t^{(k,b)} - \boldsymbol{\mu}_t)^2, \quad (5)$$

which are further used to calculate the confidence intervals of diseases, as described below.

Decision Threshold. Intuitively, doctors stop inquiring to inform diseases when they are *confident* that inquiring

more symptoms would not overturn his diagnosis. Therefore, we propose the decision threshold (DT) to mimic such introspective process, that is, the agent would stop inquiring to inform the preferred disease *if the agent believes that the probability of the preferred disease is high enough so that inquiring more symptoms would not overturn the preferred disease probabilistically*. In other words, DT would be met if the probability of the preferred disease is beyond the upper bound of the 6σ confidence interval [35], [36] of the other diseases' probabilities (step 8 in Fig. 4). Denote the preferred disease as i , i.e., $i = \text{argmax}_j \mu_t^{(j)}, \forall j \in [1, m]$. DT is formulated as

$$\text{DT}(\boldsymbol{\mu}_t, \boldsymbol{\sigma}_t) = \begin{cases} \text{True}, & \forall j \neq i, \mu_t^{(i)} > \mu_t^{(j)} + 3\sigma_t^{(j)}, \\ \text{False}, & \text{otherwise} \end{cases}. \quad (6)$$

4.3.2 Inquiry Branch

The diagnosis branch depends on the inquiry branch to explore the meaningful symptoms. The latter branch follows the Q network [23], which takes the concatenation of the state s_t and the current disease probabilities \mathbf{u}_t to predict the action a_t (step 1-2 in Fig. 4).

$$a_t = \max_a Q(s_t, \mathbf{u}_t, a; \theta). \quad (7)$$

The parametrized policy is trained by following the gradient:

$$\begin{aligned} \nabla_\theta L = & \mathbb{E}_{s_t, \boldsymbol{\mu}_t, a_t, s_{t+1}, \boldsymbol{\mu}_{t+1}} \left[\left(r_t + \gamma \max_a Q(s_{t+1}, \mathbf{u}_{t+1}, a; \theta_{\text{targ}}) \right. \right. \\ & \left. \left. - Q(s_t, \mathbf{u}_t, a_t; \theta) \right) \nabla_\theta Q(s_t, \mathbf{u}_t, a_t; \theta) \right], \end{aligned} \quad (8)$$

where the parameter θ_{targ} represents the target Q network updated with the Polyak factor α to stabilize the training,

$$\theta_{\text{targ}} = \alpha \theta_{\text{targ}} + (1 - \alpha) \theta. \quad (9)$$

4.3.3 Reward for a single goal

Existing RL methods [6], [7] design a complex reward function to train the policy to maximize the accumulated rewards. However, the design of reward is sensitive to different scenarios, making the meaning of the accumulated rewards too complex to be understood. By disentangling the disease-diagnosis from the policy, the goal of the policy becomes more specific: meeting DT as soon as possible. Therefore, the reward of our policy is set as a constant $r_t = -0.1$ to encourage the agent to meet DT as soon as possible.

5 EXPERIMENTS

In this section, we evaluated our CSMAD methodology on two MAD benchmarks, i.e., MuZhi (**MZ**) [7] composed of 586 training and 142 test records with 66 symptoms and 4 diseases; DingXiang (**DX**) [6] composed of 423 training and 104 test records with 41 symptoms and 5 diseases. More details about the experiments are placed in the Appendix C. $\mathcal{P}^{\text{train}}$ and \mathcal{P}^{all} denote the patient simulators organized by the training records and all records (records for training and testing) in a benchmark respectively. For instance, $\mathcal{P}_{\text{PBPS}}^{\text{train}}$ represents the PBPS using training records in a benchmark to interact with the agent. In our experiments, we sought

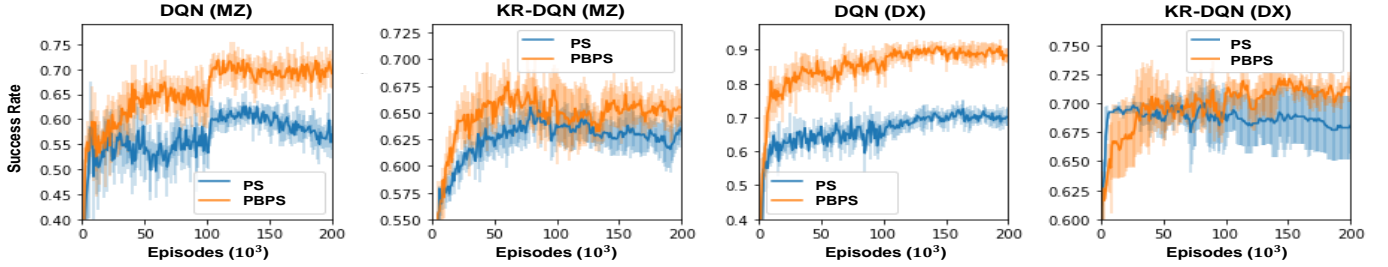


Fig. 5: The success-rate curves of the original patient simulator (PS) and our probabilistic-symptom patient simulator (PBPS) based on DQN [7] and KR-DQN [6] trained in the benchmarks MZ and DX, respectively.

TABLE 1: RR and SD of the patient simulators across benchmarks.

Benchmarks	Indexes	PS [6], [7]	GEN [32]	PBPS
MZ	CD	0.6028	0.6563	0.7746
	SD	0.085	0.081	0.426
DX	CD	0.7308	0.7212	0.7789
	SD	0.116	0.110	0.438

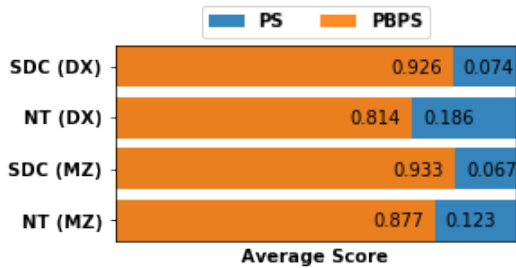


Fig. 6: The comparison of human evaluation on PS and PBPS across benchmarks.

to answer the following questions: **1)** *Is the propensity-based patient simulator able to generate more informative and disease-related answers for counterfactual symptom inquiries?* **2)** *How data-efficient and robust of our P2A in comparison with other baselines?*

Unless stated otherwise, all evaluation curves are generated by averaging the *success rates* (the test accuracy in diagnosis) of **five runs** with different random seeds, and their shadow areas denote the standard deviation.

Baselines. To answer the first question, we have compared PBPS with PS [6], [7] and a generative world model (GEN) [32]. GEN is trained with Equ. (3) like PBPS, while PBPS conducts further propensity score matching. As for the second question, we compared our P2A against three baselines using PBPS, i.e., DQN [7], KR-DQN [6] and supervised learning (SL). DQN combines symptom-inquiry and disease-diagnosis into a single policy network and train it by deep q-learning [21], [22]. KR-DQN [6] adds a knowledge-routing module at the head of the policy using predefined disease-symptom knowledge. Distinguished from DQN and KR-DQN, P2A disentangles the disease-diagnosis from the policy. SL uses supervised learning to train bootstrapping classifiers using the same structure as the bootstrapping classifiers in P2A. Note that for SL, we force the agent to inquire all of the symptoms from PBPS during training and testing, and then use the final state as its input.

5.1 Evaluation on PBPS

We propose two evaluation metrics to measure the patient simulators by quantifying how informative and disease-related their answers are. The first metric *Coincidence Degree* (CD) describes the test accuracy of the classifier trained with the $\mathcal{P}^{\text{train}}$. In the training phase of CD, an input instance is generated by inquiring random symptoms of a random size from $\mathcal{P}^{\text{train}}$. The higher CD means that the answers of the simulator are more likely to imply the actual symptom-disease relation, and therefore the agent learning with the simulator can diagnose better. The second metric *Symptom Density* (SD) represents the proportion of informative values (-1 or 1) in the full states from the patient simulator. The higher SD means the simulator is more likely to answer an inquiry informatively.

Quantitative evaluation. We calculated CD and SD among $\mathcal{P}_{\text{PS}}^{\text{train}}$, $\mathcal{P}_{\text{GEN}}^{\text{train}}$ and $\mathcal{P}_{\text{PBPS}}^{\text{train}}$. As shown in Tab. 1, PBPS has obtained the highest score in both CD and SD, meaning that PBPS can generate more informative and disease-related answers. Especially, SD of PBPS is almost four times larger than the others. In the meanwhile according to the higher CD, the increased information is consistent with the ground-truth symptom-disease relation, if not better than the original information.

Human evaluation. However, these metrics are hard to tell which simulator is more informative like the human patient and which simulator is more capable of generating disease-related answers in the view of the human doctor. Therefore, we also conducted human evaluation between PS and PBPS. We invited six human doctors to interact repeatedly with $\mathcal{P}_{\text{PS}}^{\text{all}}$ and $\mathcal{P}_{\text{PBPS}}^{\text{all}}$, and score the *Naturality* (NT, whose answers are informative like the human patient) and the *Symptom-Disease Consistency* (SDC, whose answers are more disease-related) for each simulator per evaluation episode. More details about the human evaluation are provided in Appendix C. As observed in Fig. 6, the averaging NT and SDC of PBPS have exceeding the PS sharply, which means in the view of human experts, PBPS can generate more informative and disease-related answers.

Performance improvement of MAD agents. As the answers from PBPS are more realistic, we have verified whether PBPS can be more beneficial to existing RL baselines than the original simulator. In specific, we take $\mathcal{P}^{\text{train}}$ to interact with the DQN and KR-DQN agents to train their policies, then, we evaluate their success rates on the diagnosis episodes generated by completing the absent value of the symptoms in the test set of the MAD benchmarks.

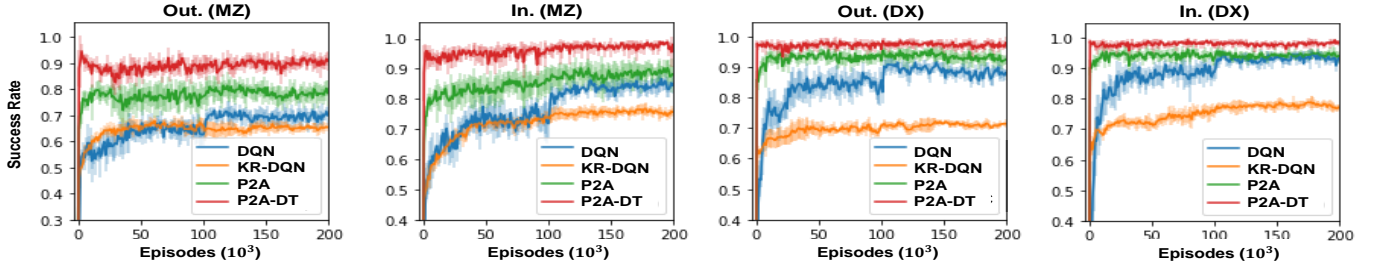


Fig. 7: The comparison of DQN, KR-DQN and P2A in MZ and DX across In./Out. evaluation settings. The curves denote the mean of the success rate over iterations with deviations.

TABLE 2: The evaluations based on MAD success rate of the dialogue, across different RL baselines in In./Out. settings.

Benchmark	Setting	DQN	KR-DQN	P2A
MZ	Out.	0.697	0.653	0.784
	In.	0.845	0.755	0.888
DX	Out.	0.880	0.709	0.928
	In.	0.932	0.777	0.944

TABLE 3: The evaluations based on MAD success rate of the dialogue, across different RL baselines in In./Out. settings.

Benchmark	Setting	P2A-direct	P2A-direct-DT	SL	P2A-DT
MZ	Out.	0.696	0.716	0.845	0.907
	In.	0.864	0.879	0.942	0.977
DX	Out.	0.840	0.857	0.952	0.971
	In.	0.920	0.933	0.962	0.982

Fig. 5 showcases the comparisons between the PS and PBPS based on success rates across RL baselines and benchmarks. We have observed that when trained with the episodes generated by PBPS, the RL baselines reap a significant performance over the original. It evidences that using PBPS helps to develop more competitive MAD agents for real-world applications.

5.2 Evaluation on P2A

As we have answered the first question, we propose empirical studies to demonstrate the superiority of our P2A agent to answer the second question. The evaluated baselines trained with \mathcal{P}_{PBPS} , including DQN, KR-DQN, and P2A, are evaluated in two settings: In-distribution (In.) and Out-of-distribution (Out.). In the In. setting, the dialogue episodes used for training and testing are all generated by interacting with \mathcal{P}_{PBPS}^{all} . In the Out. setting, the training dialogue episodes is generated from $\mathcal{P}_{PBPS}^{train}$, then the trained RL agents are tested by interacting with \mathcal{P}_{PBPS}^{all} . All the test simulated patients are invisible during training. The first setting aims to testify the basic MAD performances of the RL agents since the training episodes and testing episodes are generated from the same distribution. On the contrary, the second setting is to verify the cross-distribution generalization abilities of the RL agent. Note that, since the decision threshold is not always met in each dialogue episode, we define a limit of the number of the interactions in case the agent traverses all the symptoms, degenerating the active symptom-inquiry into a form-filling manner. To demonstrate the power of the decision threshold, we also measure the success rate of P2A where DT is satisfied (P2A-DT).

Fast convergence and reliable diagnosis. Fig.7 illustrates the success rate over the iteration of the training episodes required to train the RL agents. P2As (P2A and P2A-DT) achieve faster convergence and higher success rate upper bounds than all other baselines. Remarkably, those episodes that met the DT achieve a very high success rate even at the very beginning of the training phase (red curve),

meaning that DT only needs a small amount of training data to work reliably. Such reliable diagnosing performance is significant especially in MAD task as the data are expensive to collect.

More accurate and robust diagnosis across In./Out. settings. In Tab.2, we compare different baselines by evaluating the mean success rate over the last 20,000 training episodes. P2A outperforms the other RL baselines with a clear margin in either In. or Out. setting. Ought to be regarded that, DQN and KR-DQN perform very sensitively when the patient simulators are different for training and testing (the Out. setting). KR-DQN use the predefined symptom-disease relation as prior, which might be not generalized well to PBPS. In comparison, P2A is affected less in the change of the distributions. It means that disentangling the disease-diagnosis and posing assurance check (DT) help the agent make robust diagnoses.

Effective two-step model and Decision Threshold. As mentioned in the first paragraph in Sec. 4.3.1, using a two-step model to model $P(d|s_t)$ is more in line with the requirement of MAD, we here evaluated the performance of P2A without the two-step model. In Tab. 3, we can observe that the performance of P2A without two-step model, i.e., P2A-direct/P2A-direct-DT, is severely affected. We have also evaluated the performance of SL. The performance of SL is better than almost all RL baselines since it can observe all symptom information during training and testing. However, the performance of P2A-DT is better than SL overwhelmingly with partial observation. Especially in the Out. setting, the success rate of P2A-DT is consistently exceeding 0.9. It means that the DT can work reliably without knowing all information even to the unfamiliar patient situation, which is quite crucial for the real-world scenario.

6 CONCLUSION

This paper presented a complete RL framework for MAD task, CSMAD, including a patient simulator PBPS that takes the advantages of PSM to tackle the problem of counterfactual symptom inquiry, and an MAD agent P2A that

additionally models the confidence to drive the symptom-inquiry. Experimental results demonstrate that PBPS can generate more informative and disease-related answers from both quantitative and qualitative aspects. And the P2A agent is more sample-efficient and robust. Our introduced Decision Threshold provides a reliable stop mechanism for MAD agent across various settings. In future work, we will improve the simulator by incorporating more powerful techniques from natural language processing, e.g., exploiting the rich context for each record of symptoms and diagnoses. And introducing causal inference with the reinforced agent training can be another possibility.

APPENDIX A

PROPENSITY-BASED PATIENT SIMULATOR (PBPS)

A.1 Propensity Score Matching (PSM)

In real life, we can only observe the outcome of the actual action, which is named as the factual outcome. However, sometimes we might wonder what the outcome should have been if the other action had been taken, that is the counterfactual outcome. The potential outcome can be either factual or counterfactual. According to the potential outcome framework [12], [13], the counterfactual outcome is inferrable if the three assumptions are met: the stable unit treatment value assumption (SUTVA), consistency and ignorability (unconfoundedness). Ordinarily, SUTVA and consistency are assumed to be satisfied. With ignorability, we assume that all the confounding variables are observed and reliably measured by a set of features $X^{(u)}$ for each instance u . $X^{(u)}$ denotes a set of confounding variables, namely a subset of features that describes the instance u and causally influences the values of both the treatment $A^{(u)}$ and the potential outcome $Y_a^{(u)}$. Ignorability means that the values of the potential outcomes $Y_a^{(u)}$ are independent of the factual action $A^{(u)}$, given $X^{(u)}$. Mathematically, ignorability can be formulated as:

$$Y_a^{(u)} \perp\!\!\!\perp A^{(u)} | X^{(u)}. \quad (10)$$

From the notation, we can see that this is an assumption defined at the individual level. With ignorability satisfied, we can estimate the counterfactual outcome of u through the factual outcomes of other instance u' with the same covariates $Y_a^{(u)} = Y_a^{(u')} | X^{(u)} = X^{(u')}$, which is the essence of *the matching methods* [14].

However, we need to be careful when there exists a group which only contains instances with only one type of action. We cannot estimate the counterfactual outcome in this group. This issue is referred to as *the lack of overlap*. To overcome this issue, the most widely adopted matching as weighting methods specify the function $e(X^{(u)})$ in estimating *propensity score* $P(A^{(u)} | X^{(u)})$ [?]. We need to make sure whether the ignorability still holds with $e(X^{(u)})$. In other words, given $e(X^{(u)})$, whether the $Y_a^{(u)} \perp\!\!\!\perp A^{(u)} | e(X^{(u)})$ still holds. We show that $Y_a^{(u)} \perp\!\!\!\perp A^{(u)} | e(X^{(u)})$ is satisfied in the following. Here, for brevity, (Y, X, A) denotes $(Y_a^{(u)}, X^{(u)}, A^{(u)})$.

$$\begin{aligned} P(A|e(X)) &= \mathbb{E}[A|e(X)] = \mathbb{E}[\mathbb{E}[A|X, e(X)]|X] \\ &= \mathbb{E}[\mathbb{E}[A|X]|X] = \mathbb{E}[e(X)|X] = e(X) \end{aligned} \quad (11)$$

$$\begin{aligned} P(Y, A|e(X)) &= P(Y|e(X))P(A|Y, e(X)) \\ &= P(Y|e(X))\mathbb{E}[P(A|Y, e(X), X)|X] \\ &= P(Y|e(X))\mathbb{E}[P(A|Y, X)|X] \\ &= P(Y|e(X))\mathbb{E}[P(A|X)|X] \quad \text{by ignorability (12)} \\ &= P(Y|e(X))\mathbb{E}[e(X)|X] \\ &= P(Y|e(X))e(X) \\ &= P(Y|e(X))P(A|e(X)) \quad \text{according to (11)} \end{aligned}$$

From (12), we know that $Y_a^{(u)} \perp\!\!\!\perp A^{(u)} | e(X^{(u)})$. It means that we can estimate the counterfactual outcome of u by matching instances with the same propensity score $e(X^{(u)})$.

A.2 Details of PBPS

To show that PSM is workable in our patient simulator, we need to show the ignorability is satisfied given the covariates $X^{(p)} = (\mathbf{y}^{(p)}, d^{(p)})$ of the record p , i.e., $Y_a^{(p)} \perp\!\!\!\perp A^{(p)} | (\mathbf{y}^{(p)}, d^{(p)})$, where $Y_a^{(p)}$ and $A^{(p)}$ is the random variables for the potential existence of symptom and the factual symptom inquiry, $\mathbf{y}^{(p)}$ is the observed symptoms and $d^{(p)}$ is the ground-truth disease of the record p . A reasonable assumption is that the symptom inquiry $A^{(p)}$ is only dependent on the history observed symptoms $\mathbf{y}^{(p)}$, and the existence of symptom $Y^{(p)}$ is only dependent on the disease $d^{(p)}$. Here, for brevity, (Y, A, \mathbf{y}, d) denotes $(Y_a^{(p)}, A^{(p)}, \mathbf{y}^{(p)}, d^{(p)})$. Then we have

$$P(Y, A|\mathbf{y}, d) = P(Y|d)P(A|\mathbf{y}) = P(Y|\mathbf{y}, d)P(A|\mathbf{y}, d). \quad (13)$$

From (13), we know that the ignorability $Y_a^{(p)} \perp\!\!\!\perp A^{(p)} | (\mathbf{y}^{(p)}, d^{(p)})$ holds. According to the PSM, the propensity score in AD could be $e(\mathbf{y}^{(p)}, d^{(p)}) = P(A^{(p)} | \mathbf{y}^{(p)}, d^{(p)})$. Nevertheless, we not only want the probability of symptom inquiry to be matched but also the symptom existence to be matched. To this, we adopt a more strict propensity score

$$\begin{aligned} P(Y_a|\mathbf{y}, d) &= P(A, Y_A|\mathbf{y}, d) = P(A|\mathbf{y}, d)P(Y_A|A, d) \\ &= e(\mathbf{y}, d)P(Y_A|A, d). \end{aligned} \quad (14)$$

Again, $Y_a^{(p)} \perp\!\!\!\perp A^{(p)} | P(Y_a|\mathbf{y}, d)$ is satisfied because matching $P(Y_a|\mathbf{y}, d)$ implies matching $e(\mathbf{y}^{(p)}, d^{(p)})$. Assuming the symptom existence is only dependent on the disease d , then the propensity score for all symptoms is $f(\mathbf{y}, d) = P(\mathbf{Y}|\mathbf{y}, d)$

The multi-classifier adopted for training the propensity score $f_{\phi_P}(\mathbf{y}, d)$ with parameter ϕ_P is shown in Fig. 8, whose intermediate result $f_{\hat{\phi}_P}(\mathbf{y}, d)$ from the second to the last FC layer is used as the patient propensity score as it's more compact. The input dimension i is set as $m + n$ and the output dimension o is set as n , where m is the number of diseases, and n is the number of symptoms. During training, the input is masked with a random binary mask \mathbf{m} resulting in $(\mathbf{y} \odot \mathbf{m}, d)$, and the target is to recover the original information \mathbf{y} . Given the anchor record p , we first calculate the propensity scores of the other records q . Since for the anchor p , the observed covariates is $(\mathbf{y}^{(p)}, d^{(p)})$. Therefore, we only match the anchor record with the others ignoring the unobserved symptoms. Thus, the propensity of q according to p is $f_{\hat{\phi}_P}(\mathbf{y}^{(q)} \odot \mathbf{m}^{(p)}, d^{(q)})$, where $\mathbf{m}^{(p)} = \mathbb{I}(y_a \neq 0, \forall a \in [1, \dots, n])$. The similarity weight

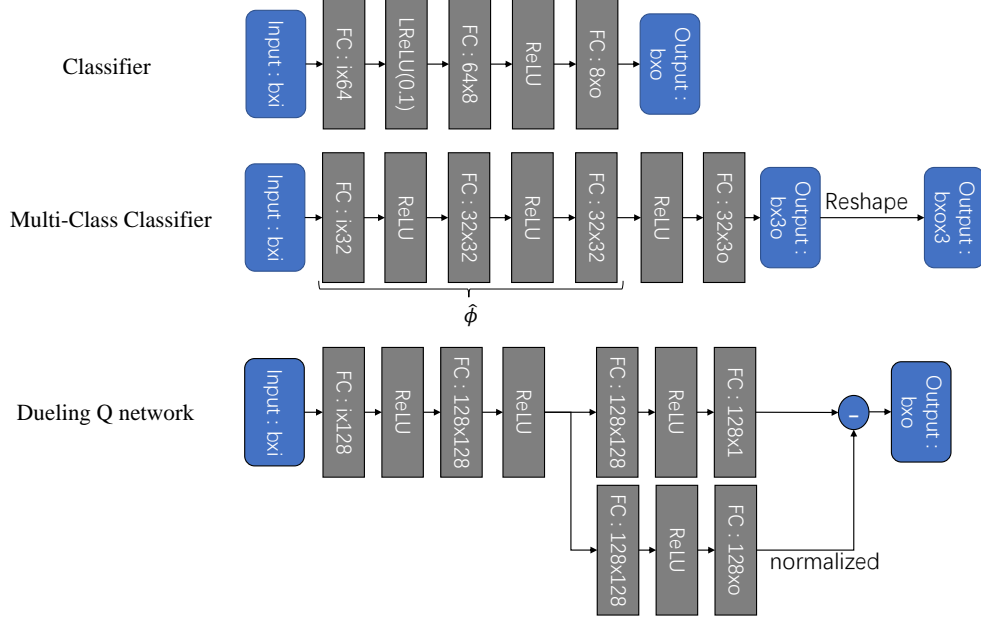


Fig. 8: Two types of network structures used throughout the whole work, i.e. “Classifier” (upper) and “Multi-Class Classifier” (lower). “FC” is the abbreviated form of a fully connected layer, and “LReLU (0.1)” is the abbreviated form of leaky ReLU activation with a negative slope as 0.1. b denotes the batch size of the input and i denotes the input dimension.

$P(q|p, a)$ is then calculated according to $f_{\hat{\phi}_P}(\mathbf{y}^{(p)}, d^{(p)})$ and $f_{\hat{\phi}_P}(\mathbf{y}^{(a)} \odot \mathbf{m}^{(p)}, d^{(a)})$.

APPENDIX B PROGRESSIVE ASSURANCE AGENT (P2A)

B.1 Details of P2A

B.1.1 Generative sampler

Similar to the PBPS, we adopt the multi-classifier network in Fig. 8 for the final state generator. This generative model is aimed at predicting the final state \hat{s}_t of the current state s_t . Therefore, we model it as a generative problem. ϕ_G is the parameter of the generator $f_{\phi_G}(\cdot)$. The input dimension i and the output dimension o are both set as n . N is the number of final states in the buffer. The Monte Carlo sampling is applied obeying the generative model $f_{\phi_G}(s_t)$ to sample a set of possible final states $\{\hat{s}\}$.

B.1.2 Bootstrapping diagnosers

The network structure of the bootstrapping diagnoser is the classifier structure in Fig. 8. The input dimension is set as n , and the output dimension is set as m . The input \hat{s}_t is sampled from the generative sampler, and the target d is collected at the end of the episodes. During training, the training data are sampled with replacement from the data buffer, in order to eliminate the sampling bias caused by the training data sampling and focus on estimating the uncertainty of the network parameters.

B.1.3 Policy network

The Q-learning policy network we adopted is the Dueling-DQN [23] in Fig. 8 for stabilizing the training procedure, which has two heads with one for state value V and the other one for action advantage value A . Therefore, $Q(s_t, \mu_t, a_t) = V(s_t, \mu_t) + A(s_t, \mu_t, a_t)$, where μ_t is the expectation of disease probability calculated from the output

of the bootstrapping diagnosers. In order to avoid repeating choosing symptoms have been visited, we subtract 1000000 for each symptom has been inquired from the $Q(s_t, \mu_t, a_t)$ to decrease the q values of these symptoms. The input contains three vector, i.e., the state s_t , the inquired history $[\mathbb{I}(s_{t,a} \neq -2), \forall a \in [1, \dots, n]]$ and the expectation of diseases’ probabilities μ . Therefore the input dimension i is set as $2 \times n + m$ and the output dimension o is set as n .

APPENDIX C EXPERIMENT DETAILS

C.1 Training Details

For training the propensity score estimator of PBPS, the learning rate is 0.01 initially and is decreased to the tenth of it for every 10000 iterations. The total training iterations is 40000 with Adam optimizer. The batch size b is 128.

For training the P2A, the learning rate of the policy network is 0.001 and is decreased to the tenth of it after 100,000 training episodes while the learning rate for the generative sampler and the bootstrapping diagnosers is fixed at 0.001. All of the parameters are updated by Adam optimizer. The maximum number of training episodes is 200,000. The max dialogue rounds T is $1/3 \times N$. The constant reward -0.1 is given to the agent for each round to encourage the shorter dialogues. The ϵ of ϵ -greedy strategy is set to 0.1 for efficient action space exploration, and the discount factor γ in the Bellman equation is 0.95. The size of buffer D_Q is 50,000 and the size of buffer D_C is 1280. The batch size is 32, and the Polyak factor is 0.99. The number of samples of the generative sampler is set as 50, and the number of the bootstrapping models is 10. We update the target policy every ten rounds and update the model every round after 6,000 random start rounds.

C.2 Baselines details

The RL baselines DQN [7] and KR-DQN [6] are trained with the open-source code from KR-DQN [6] with default training settings. The classifier structure of "SL" is the same as the diagnosers of P2A. For training the "SL", the training input is augmented by the random binary mask \mathbf{m} , which we found could enhance the test accuracy. Moreover, the batch size for training is set as 32, and the learning rate is 0.001, which will decrease to the tenth of it after every 40000 iterations with Adam optimizer. The total training iterations is set as 100000. In order to train the model "SL" for a given patient simulator, we sample 30000 full states by inquiring all symptoms from the patient simulator as the training data.

C.3 Evaluation for Patient Simulator

C.3.1 Quantative evaluation details

In order to evaluate a patient simulator $\mathcal{P}^{(\text{train})}$ quantitatively. We proposed two indexes: CD and SD. To calculate them, we firstly inquire all symptoms of $\mathcal{P}^{(\text{train})}$ generate 30000 full states. For the CD of $\mathcal{P}^{(\text{train})}$, we randomly masked off some of the symptom existences of the training batch (to mimics a batch of states collected through a limited amount of inquires) to train a classifier with the same training settings as the "SL". The test accuracy of the classifier is CD. As for the SD of $\mathcal{P}^{(\text{train})}$, we calculated the proportion of non-zero symptoms of these states.

C.3.2 Human evaluation details

In order to measure the qualitative performance of the patient simulators, i.e. PS and PBPS, we propose 'Natural-ity' (NT) and 'Symptom-Disease Consistency' (SDC) metrics. NT is to score how natural the simulator is (we ask the human experts: "Which one is more natural?") and SDC is to score whether the patient simulator can generate disease-related responses (we ask the human experts: "Which one is more disease-related?"). The reason that we use NT instead of Informativity (corresponding to 'informative') is that informativity can be well quantified by the 'Symptom Density' proposed in the quantitative evaluation. Realizing that the ultimate goal of the quantitative and qualitative evaluations are to find out which patient simulator is more like a human patient. we decide to employ the more essential yet more subjective index, i.e., 'Naturality'.

The experts were required to decide which simulator is more natural (score 1) and which simulator is more disease-related (score 1) per episode with the two patient simulators. We invited six human doctors and made each doctor interact with the two patient simulators with 30 episodes (5 interactions each episode) with random anchor records from each dataset. We adopted the simple template-based natural language generator for both the patient simulators to response to the doctor's inquiry simultaneously. As for the doctors, we offered them the list of all the symptoms of each dataset. For each evaluation episode, one random anchor record was chosen for both the patient simulators, and the doctors were provided with the self-report and the corresponding ground truth disease of the anchor record. Then the doctor would initiate inquiries about symptoms which were answered by both patient simulators without knowing which answer is from which patient simulator.

After interviewing, we counted the proportion of NT and SDC for each patient simulator by dividing the total number of samples, i.e. 6×30 (6 doctors and 30 samples for each dataset and each patient simulator).

REFERENCES

- [1] K.-F. Tang, H.-C. Kao, C.-N. Chou, and E. Y. Chang, "Inquire and diagnose: Neural symptom checking ensemble using deep reinforcement learning," in *NeurIPS*, 2016.
- [2] Z. Lipton, X. Li, J. Gao, L. Li, F. Ahmed, and L. Deng, "Bbq-networks: Efficient exploration in deep reinforcement learning for task-oriented dialogue systems," *AAAI*, 2018.
- [3] T. Wen, D. Vandyke, N. Mrkšić, M. Gašić, L. Rojas-Barahona, P. Su, S. Ultes, and S. Young, "A network-based end-to-end trainable task-oriented dialogue system," in *ACL*, 2017.
- [4] Z. Yan, N. Duan, P. Chen, M. Zhou, J. Zhou, and Z. Li, "Building task-oriented dialogue systems for online shopping," in *AI*, 2017.
- [5] R. Lowe, N. Pow, I. V. Serban, and J. Pineau, "The ubuntu dialogue corpus: A large dataset for research in unstructured multi-turn dialogue systems," in *SIGDD*, 2015, p. 285.
- [6] L. Xu, Q. Zhou, K. Gong, X. Liang, J. Tang, and L. Lin, "End-to-end knowledge-routed relational dialogue system for automatic diagnosis," *AAAI*, 2019.
- [7] Z. Wei, Q. Liu, B. Peng, H. Tou, T. Chen, X. Huang, K.-F. Wong, and X. Dai, "Task-oriented dialogue system for automatic diagnosis," in *ACL*, vol. 2, 2018, pp. 201–207.
- [8] S. Mithen and J. Morton, "The prehistory of the mind," 1996.
- [9] Y. N. Harari, *Sapiens: A brief history of humankind*. Random House, 2014.
- [10] J. Pearl, "Theoretical impediments to machine learning with seven sparks from the causal revolution," in *ICWSDM*, 2018.
- [11] M. A. Hernán, J. Hsu, and B. Healy, "A second chance to get causal inference right: a classification of data science tasks," *Chance*, vol. 32, no. 1, pp. 42–49, 2019.
- [12] D. B. Rubin, "Estimating causal effects of treatments in randomized and nonrandomized studies," *JEP*, vol. 66, no. 5, p. 688, 1974.
- [13] J. Neyman, "Sur les applications de la théorie des probabilités aux expériences agricoles: Essai des principes," *Roczniki Nauk Rolniczych*, vol. 10, pp. 1–51, 1923.
- [14] E. A. Stuart, "Matching methods for causal inference: A review and a look forward," *SS*, vol. 25, no. 1, p. 1, 2010.
- [15] R. H. Dehejia and S. Wahba, "Propensity score-matching methods for nonexperimental causal studies," *RES*, vol. 84, no. 1, pp. 151–161, 2002.
- [16] P. C. Austin, "An introduction to propensity score methods for reducing the effects of confounding in observational studies," *MBR*, vol. 46, no. 3, pp. 399–424, 2011.
- [17] J. S. B. Evans, "Dual-processing accounts of reasoning, judgment, and social cognition," *ARP*, vol. 59, pp. 255–278, 2008.
- [18] J. W. Kable and P. W. Glimcher, "An as soon as possible effect in human intertemporal decision making: behavioral evidence and neural mechanisms," *JN*, vol. 103, no. 5, pp. 2513–2531, 2010.
- [19] H.-C. Kao, K.-F. Tang, and E. Y. Chang, "Context-aware symptom checking for disease diagnosis using hierarchical reinforcement learning," in *AI*, 2018.
- [20] Y.-S. Peng, K.-F. Tang, H.-T. Lin, and E. Chang, "Refuel: Exploring sparse features in deep reinforcement learning for fast disease diagnosis," in *NeurIPS*, 2018, pp. 7333–7342.
- [21] V. Mnih, K. Kavukcuoglu, D. Silver, A. Graves, I. Antonoglou, D. Wierstra, and M. Riedmiller, "Playing atari with deep reinforcement learning," *CS*, 2013.
- [22] V. Mnih, K. Kavukcuoglu, D. Silver, A. A. Rusu, J. Veness, M. G. Bellemare, A. Graves, M. Riedmiller, A. K. Fidjeland, G. Ostrovski *et al.*, "Human-level control through deep reinforcement learning," *Nature*, vol. 518, no. 7540, p. 529, 2015.
- [23] Z. Wang, T. Schaul, M. Hessel, H. Van Hasselt, M. Lanctot, and N. De Freitas, "Dueling network architectures for deep reinforcement learning," *ICML*, 2016.
- [24] P. Whaithe and F. P. Ferrie, "Autonomous exploration: Driven by uncertainty," *TPAMI*, vol. 19, no. 3, pp. 193–205, 1997.
- [25] —, "From uncertainty to visual exploration," *TPAMI*, no. 10, pp. 1038–1049, 1991.
- [26] R. McAllister, G. Kahn, J. Clune, and S. Levine, "Robustness to out-of-distribution inputs via task-aware generative uncertainty," *ICRA*, 2019.

- [27] I. Osband, J. Aslanides, and A. Cassirer, "Randomized prior functions for deep reinforcement learning," in *NeurIPS*, 2018, pp. 8617–8629.
- [28] Y. Burda, H. Edwards, A. Storkey, and O. Klimov, "Exploration by random network distillation," *ICLR*, 2019.
- [29] J. Schatzmann, B. Thomson, K. Weilhammer, H. Ye, and S. Young, "Agenda-based user simulation for bootstrapping a pomdp dialogue system," in *ACL*. *ACL*, 2007, pp. 149–152.
- [30] X. Li, Z. Lipton, B. Dhingra, L. Li, J. Gao, and Y.-N. Chen, "A user simulator for task-completion dialogues," 12 2016.
- [31] B. Dhingra, L. Li, X. Li, J. Gao, Y.-N. Chen, F. Ahmed, and L. Deng, "End-to-end reinforcement learning of dialogue agents for information access," in *ACL*, 2016.
- [32] B. Peng, X. Li, J. Gao, J. Liu, and K.-F. Wong, "Integrating planning for task-completion dialogue policy learning," in *ACL*, 2018.
- [33] H. Chen, X. Liu, D. Yin, and J. Tang, "A survey on dialogue systems: Recent advances and new frontiers," *SIGKDD*, vol. 19, no. 2, pp. 25–35, 2017.
- [34] C. M. Bishop, *Pattern recognition and machine learning*. Springer, 2006.
- [35] P. S. Pande and L. Holpp, *What is six sigma?* McGraw-Hill Professional, 2001.
- [36] E. Parzen, *Modern probability theory and its applications*. John Wiley & Sons, Incorporated, 1960.

Junfan Lin received the B.S. degree in software engineering from Sun Yat-sen University, Guangzhou, China, where he is currently working toward the Ph.D. degree in computer science and technology, advised by Prof. L. Lin. His research interests include reinforcement learning and natural language processing.

Ziliang Chen received the B.S. degree in mathematics and applied mathematics from Sun Yat-sen University, Guangzhou, China, where he is currently working toward the Ph.D. degree in computer science and technology, advised by Prof. L. Lin. His research interests include computer vision and machine learning.

Xiaodan Liang received the PhD degree from Sun Yat-sen University, in 2016, advised by Liang Lin. She is currently an Associate Professor at Sun Yat-sen University. She is also served as area chairs of CVPR 2020, ICCV 2019 and WACV 2020. She was a postdoc researcher with Machine Learning Department, Carnegie Mellon University, working with Prof. Eric Xing, from 2016 to 2018. She has published several cuttingedge projects on the human-related analysis including the human parsing, pedestrian detection and instance segmentation, 2D/3D human pose estimation and activity recognition.

Keze Wang received the B.S. degree in software engineering from Sun Yat-sen University, Guangzhou, China, in 2012. He received the dual Ph.D. degree with Sun Yat-sen University and The Hong Kong Polytechnic University under the supervision of Prof. L. Lin and L. Zhang. He is currently a postdoctoral scholar in VCLA lab at UCLA. His current research interests include computer vision and machine learning. More information can be found in his personal website <http://kezewang.com>.

Liang Lin is a Full Professor of Sun Yat-sen University. He served as the Executive R&D Director and Distinguished Scientist of SenseTime Group from 2016 to 2018, taking charge of transferring cutting-edge technology into products. He has authored or co-authored more than 200 papers in leading academic journals and conferences. He is an associate editor of *IEEE Trans*, *Human-Machine Systems* and *IET Computer Vision*. He served as Area Chairs for numerous conferences such as CVPR, ICCV and IJCAI. He is the recipient of numerous awards and honors including Wu Wen-Jun Artificial Intelligence Award, ICCV Best Paper Nomination in 2019, Annual Best Paper Award by Pattern Recognition (Elsevier) in 2018, Best Paper Dimond Award in IEEE ICME 2017, and Google Faculty Award in 2012. He is a Fellow of IET.